Original Paper

In-depth analysis of elements and properties of hydrated subsurface layers on optical surfaces of a SiO_2–BaO–B_2O_3 glass with SIMS, IBSCA, RBS and NRA

Part 2. Discussion of results[1])

Hans Bach
Schott Glaswerke, Mainz (FRG)

Klaus Großkopf
Carl Zeiss, Oberkochen (FRG)

Peter March and Friedrich Rauch
Institut für Kernphysik der Johann-Wolfgang-Goethe-Universität, Frankfurt am Main (FRG)

In the second part of this contribution it was derived from the comparison of the sputter yields with the specific energy losses within the bulk glass and within the various subsurface layers, that the differences in the matrix effects for SIMS and IBSCA between the bulk glass and the subsurface layers are caused by a decrease of the atomic densities and of the mean atomic bond energies within the subsurface layers as well. The knowledge of the matrix effects and their origin was most important for the interpretation of the SIMS and IBSCA in-depth profiles recorded for samples prepared with variations of the production parameters. E. g., various degrees of hydration and swelling could be distinguished by the influence of the different matrix effects on the in-depth profiles of the elements. The variations in the degrees of hydration of the subsurface layers could be ascribed to the influence of the thermal treatment before coating, to the interaction with slurries of different pH values and to the duration of storage before coating with $\lambda/4$-MgF_2 layers. It is of importance for the fabrication of optical surfaces that the analysis results and the optical properties of the subsurface layers could be correlated with each other and with respective changes of the production parameters.

The results illustrate that the properties of hydrated subsurface layers depend sensitively on a great variety of parameters which may be difficult to keep constant during processing. It is recommended, therefore, that such subsurface layers should be avoided whenever possible in optical fabrication to make it easier to attain the high reproducibility required for the optical properties.

Untersuchung der Element-Tiefenverteilungen und Eigenschaften hydratisierter Oberflächenschichten auf optischen Flächen eines SiO_2–BaO–B_2O_3-Glases mit SIMS, IBSCA, RBS und NRA

Teil 2. Diskussion der Ergebnisse

Im vorliegenden zweiten Teil dieser Arbeit wurden die Zerstäubungsausbeuten mit den spezifischen Energieverlusten im kompakten Glas und in den verschiedenen Oberflächenschichten miteinander verglichen. Aus diesem Vergleich konnte abgeleitet werden, daß die Unterschiede in den Matrixeffekten von SIMS und IBSCA für Glas und Oberflächenschichten durch die in den Oberflächenschichten kleineren atomaren Dichten und mittleren Bindungsenergien der Atome verursacht werden. Die Kenntnis der Matrixeffekte und ihrer Ursache war für die Deutung der mit SIMS und IBSCA erhaltenen Element-Tiefenprofile an Proben von Bedeutung, die bei Variation der Produktionsparameter erhalten wurden. So konnten z. B. Unterschiede im Hydratationsgrad und der Quellung aus dem Einfluß der unterschiedlichen Matrixeffekte auf die Element-Tiefenprofile abgeleitet werden. Die Unterschiede im Hydratationsgrad der Oberflächenschichten konnten dem Einfluß der Unterschiede in der Wärmebehandlung vor dem Aufbringen der Vergütungsschicht, der Wechselwirkung mit Polierbrühen mit unterschiedlichen pH-Werten und Unterschieden in der Lagerdauer vor dem Belegen mit $\lambda/4$-MgF_2-Vergütungsbelägen zugeschrieben werden. Für die Fabrikation optischer Flächen ist von Bedeutung, daß die Analysenergebnisse und die Messung der optischen Eigenschaften der Oberflächenschichten sowie die jeweiligen Änderungen in den Produktionsparametern jeweils miteinander korrelierbar waren.

Die Resultate zeigen, daß die Eigenschaften der hydratisierten Oberflächenschichten empfindlich von einer Vielzahl von Prozeßparametern abhängen, deren Konstanz einzuhalten schwierig sein kann. Es wird deshalb empfohlen, die Entstehung solcher Oberflächenschichten in der Fabrikation, wenn immer möglich, zu vermeiden, um die Einhaltung der verlangten hohen Reproduzierbarkeit der optischen Eigenschaften zu erreichen.

4. Discussion

4.1. Conclusions from the comparison of the results obtained with SIMS, IBSCA, NRA and RBS

Tables 4 and 5 give an overview over all the results obtained so far with the surface analysis methods applied here, together with the respective refractive indices and thicknesses of the subsurface layers under investigation (compare with part 1). The comparison of the concentrations given in the tables yields important findings:

a) The NRA results revealed a relatively great concentration of hydrogen within some of the subsurface layers.

b) According to the RBS results the concentration of barium was decreased within the subsurface layers developed by the interaction with the slurry of

Received 6 February 1986, revised manuscript 10 July 1986.
[1]) Part 1. Experimental investigations and results. Glastech. Ber. **60** (1987) no. 1, p. 21–30.

Table 4. Concentrations analyzed with different surface analysis methods for the main components within the subsurface layers developed on polished SK 16 glass with a slurry of pH = 6.2

subsurface layers	from $R = f(\lambda)$		from etch pits	compo-nents	C_{mb} in $10^{22} \cdot cm^{-3}$	C_{ml} in $10^{22} \cdot cm^{-3}$			
	n	d in nm	d in nm			IBSCA	SIMS	RBS	NRA
uncoated	1.52	190 ± 5 %	169±10 %	H	–	–	–	–	0.48
				Si	1.11	0.57	3.44	0.92	–
				Ba	0.68	0.044	0.14	0.23	–
				B	1.21	0.045	0.16	0.46	–
coated	1.44	130 ± 5 %	117±10 %	H	–	–	–	–	0.03
				Si	1.11	0.98	6.18	2.20	–
				Ba	0.68	0.023	0.13	≈ 0.05	–
				B	1.21	0.050	0.37	–	–

Table 5. Concentrations analyzed with different surface analysis methods for the main components within the subsurface layers developed on polished SK 16 glass with a slurry of pH = 8.5

subsurface layers	from $R = f(\lambda)$		from etch pits	compo-nents	C_{mb} in $10^{22} \cdot cm^{-3}$	C_{ml} in $10^{22} \cdot cm^{-3}$			
	n	d in nm	d in nm			IBSCA	SIMS	RBS	NRA
uncoated	1.53	150 ± 5 %	159±10 %	H	–	–	–	–	0.05
				Si	1.11	0.72	3.20	–	–
				Ba	0.68	0.018	0.13	–	–
				B	1.21	0.037	0.11	–	–
coated	1.52	88 ± 5 %	89±10 %	H	–	–	–	–	0.9
				Si	1.11	0.96	4.93	–	–
				Ba	0.68	0.037	0.16	–	–
				B	1.21	0.078	0.36	–	–

pH = 6.2. A decrease of the barium concentration can be assumed qualitatively also for the subsurface layers developed with a slurry of pH = 8.5, according to the SIMS and IBSCA results and the smaller refractive indices compared to those of the bulk.

c) The concentration of boron in the subsurface layers was decreased, too. This is indicated – though only qualitatively – by the fact that the values for the $^{11}B^+$ secondary ion currents and the excited B I emission at $\lambda = 249.7$ nm observed during the sputtering removal of the subsurface layers were much smaller than in the bulk.

The findings a) to c) are in qualitative agreement with what is known already about the interaction of barium- and boron-containing glasses with aqueous solutions. During the interaction with adjacent aqueous solutions Ba^+ and B^+ ions can be exchanged against hydronium ions, see e. g. [3, 4, 6 and 42]. Therefore, though it cannot be decided from the analysis given here whether the hydrogen was present as molecular water or whether it was incorporated as Si–O–H groups, the leached layers will also be called hydrated in the following. The balance between the dissolution rate of the glass network and the rate of the interdiffusion for the components determines the thickness of the subsurface layer and the concentration of the components, see e. g. [5 to 8].

Moreover, most important conclusions can be drawn for the first time from the comparison of the concentrations of silicon and hydrogen. This will be discussed in detail for the results of the leached layers developed with pH = 6.2 given in table 4:

d) The silicon concentration was distinctly lower than in the bulk glass for the uncoated subsurface layers leached at pH = 6.2 and was about that of fused silica for the coated one.

e) A comparison of the true silicon concentration with the ratios $Q_{Si}^{+} = i_{Sib}^{+}/i_{Sil}^{+}$ shows that the ionization coefficient p_{Sil}^{+} within the subsurface layers was much greater than that for the bulk glass and caused a strong matrix effect (different from what was assumed in section 3.1.2., part 1). This matrix effect for silicon was responsible for the distortion of the true in-depth profiles of silicon (the recorded profiles showed a much higher Si^+ secondary ion current in the subsurface layer than within the bulk, see part 1, figures 2a and b, e. g.).

f) From the comparison with the NRA results for the hydrogen concentration it can be concluded that the SIMS matrix effect for silicon was due to the hydration of the subsurface layer.

g) The results obtained for barium by RBS compared with those obtained with IBSCA suggest that a matrix effect for IBSCA also existed and that the excitation

coefficient $\alpha_{\lambda,Ba}$ showed a distinctly smaller value within the hydrated material compared to the bulk.

h) The silicon concentrations derived from the IBSCA results and the RBS results (see table 4) show that the excitation coefficient of the sputtered neutral atoms $\alpha_{\lambda,Si}$ was smaller for the leached layer than for the bulk. From the comparison of the results listed in table 4 it can also be concluded that the matrix effect is smaller for IBSCA than for SIMS within the leached layer when the recombination radiation of neutral silicon atoms is recorded.

i) From d) to h) it can be concluded that the matrix effects for SIMS and IBSCA are generally different from each other within the bulk and also within the leached layers. The ionization coefficients p_m^+ are greater, the excitation coefficients $\alpha_{\lambda,m}$ of the neutral atoms, however, are smaller within the hydrated subsurface layer than in the bulk. For the radiation emitted by the sputtered neutral cationic species a much smaller matrix effect is observed for IBSCA than for SIMS. This is in qualitative agreement with the finding that the sputtered neutral species represent the true composition better than the sputtered ionized one, see [43] and section 4.2.

Further details of the overview on the results given in tables 4 and 5 deserve special interest here: According to the NRA analysis the concentration of hydrogen was much greater within the subsurface layer developed with a slurry of pH = 6.2 prior to coating than after coating, see figures 6a and b, part 1. This will be discussed in detail in section 4.4.

It is obvious that the far higher concentration of hydrogen within the coated subsurface layer developed with pH = 8.5 compared to that developed with pH = 6.2 was not reflected by a correspondingly greater increase of the degree of ionization, see figure 6b and the Q_H^+ ratios in tables 1 and 2 in part 1. For this specimen the ratio of the concentrations for hydrogen analyzed with NRA prior to coating ($0.05 \cdot 10^{22}\,cm^{-3}$) and after the coating ($0.9 \cdot 10^{22}\,cm^{-3}$) was about $5.5 \cdot 10^{-2}$, see table 5. This ratio was distinctly smaller than the ratio of the respective secondary ion currents within the subsurface layers which can be obtained from table 2, part 1, as i_H^+ (uncoated)/i_H^+ (coated) = 1.69. This difference between these ratios lets suggest that a part of the hydrogen held within the subsurface layer below the coating did not influence the ionization coefficients and therefore did not contribute to the secondary ion currents. From the findings of other authors one can speculate whether only that part of hydrogen which was bound in an ionic bond could contribute to the production of $^1H^+$ ions [23] and another part was present within the leached layer as molecular water.

The concentrations listed in table 4 let conclude that for barium, boron and silicon the IBSCA analysis yielded distinctly smaller values than the true concentrations and those derived from SIMS for the coated and the uncoated layer at pH = 6.2. The deviations of the SIMS results from the RBS results are also not within the limits of error for both the uncoated and the coated subsurface layers.

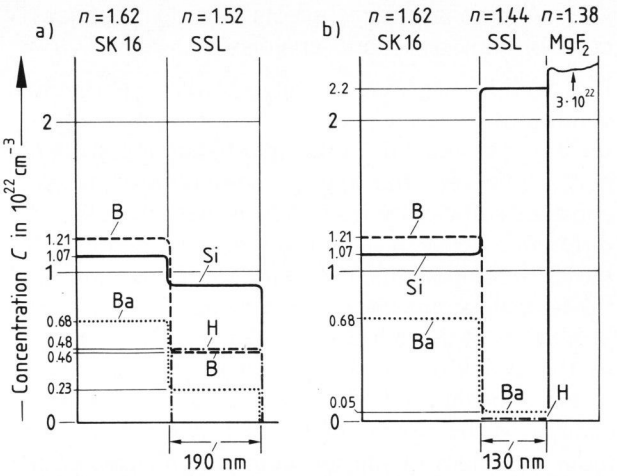

Figures 7a and b. In-depth concentration profiles for hydrogen, silicon, barium and boron derived from the results of the surface analysis methods, for the subsurface layers developed with pH = 6.2 after 6 h, a) for the uncoated specimen, b) after coating with a $\lambda/4$-MgF_2 layer.

Table 4 shows that the detection sensitivity of SIMS was distinctly greater than for IBSCA. The results derived from RBS and NRA given in table 4 allow to give quantitatively the in-depth distribution for hydrogen, silicon, barium and boron for the uncoated and coated subsurface layers developed with pH = 6.2. In figures 7a and b these in-depth distributions are shown. It should be mentioned that the values for boron were derived from the SIMS results. The latter are supposed to indicate that the ratios of the barium and boron concentrations are the same as in the bulk glass; for a support to this assumption, see section 4.4.

For all these considerations given so far, one should keep in mind that the errors of NRA and RBS analysis do not exceed 10 and 20 %, respectively. Also the errors of the calculated values given in tables 4 and 5 for SIMS and IBSCA do not exceed 15 % because the errors of the Q_m^I and Q_m^+ values, see tables 1 and 2 in part 1, reached 13 % and the ratios of the sputter rates were about 10 % erroneous.

In principle, surface potentials can affect the ratios of the ablation rates given in tables 1 and 2, part 1, and the sputter yields given in tables 4 and 5; see [24, 25 and 44] and section 2. in part 1 and the discussion on the distortion of the H^+ profile in section 4.3. Deviations by up to 20 % from the average ratios given in tables 1 and 2, part 1, were found when the discharging conditions were changed intentionally. Such an influence was ruled out by adjusting the discharging electron beam (see section 2.1., part 1).

4.2. Additional matrix effects due to changes of compositions and bond energies

It is well-known that a change in the experimental conditions can change the ionization coefficients p_m^+, see e. g. [45 and 46]. In the investigations considered here, however, the sputter conditions were kept constant sufficiently well. Accordingly the observed difference between the ionization coefficients p_m^+ for the glass components, within the subsurface layer and the bulk glass, must be due to a change of the material properties of the subsurface layers which was caused by the attack of the slurry. It has been reported in recent contributions, see e. g. [22, 23 and 46], that a change of the stoichiometry of a given matrix can induce changes of the ionization coefficients of the components. It is well-known that a greater oxygen content of metals will be connected with an increase of the ionization coefficient [20, 43 and 47] and models have been developed to understand these findings [47 and 48]. The increase of p_m^+ does not depend on whether the sample was oxidized while oxygen was implanted during sputtering or was oxidized already before [49].

Also for IBSCA a matrix effect for the excitation coefficients $\alpha_{\lambda,m}$ was reported, for a review see [50]. For the excitation of the sputtered atoms a model was developed by Kelly [51]. According to the experimental results and the models developed for describing the degree of ionization, the masses of the interacting target atoms and projectile ions and the mean atomic bond energies of the bombarded oxides influence the ionization coefficients [47, 48 and 52].

During the formation of the subsurface layers, described in part 1, an interdiffusion of Ba^+ and B^+ ions with H_3O^+ ions occurs and water can be formed by condensation [29 and 30] or can penetrate into the subsurface layers [28]. This change of the composition connected with the introduction of hydrogen could also contribute to the increase of the ionization coefficients.

Based on the various results given in section 3., part 1, and in tables 4 and 5, it may be inferred that the differences between the ionization and excitation coefficients for the bulk glass and the subsurface layers considered here can be due to changes of the compositions and of the bond energies as well. The differences between the bond energies of the bulk and the different subsurface layers can be deduced from the differences in the sputter yields and the respective specific energy losses, as will be pointed out in the following.

It has been found previously that for the sputter yields S of glasses and oxides approximately the following relation applies

$$S \sim \frac{\mathrm{d}E/\mathrm{d}x}{N\,U_B} \tag{7}$$

where $\mathrm{d}E/\mathrm{d}x$ is the specific energy loss by nuclear collisions, N is the number density of the oxides or glass atoms; for U_B the mean lattice energy per atom was taken into calculation and it was derived that this quantity was a rather good approximation for the mean bond energies of the atoms within glasses of comparable composition too [39 and 40] (for further results on the sputtering of other materials, see [53], and on the theory of sputtering of multicomponent material, see [54 and 55]). Based on equation (7) the ratios U_{Bl}/U_{Bb}, where l denotes the leached layers and b the bulk glasses, can be calculated approximately with

$$\frac{U_{Bl}}{U_{Bb}} \approx \frac{S_b(\mathrm{d}E/\mathrm{d}x)_l}{S_l(\mathrm{d}E/\mathrm{d}x)_b} \cdot \frac{N_b}{N_l} \tag{8}$$

when the total sputter yields and the specific energy losses for the two materials are known and if a correction for the different masses and bond energies, see [54 and 55], can be neglected. The ratios of the total sputter yields can be calculated with the ratios $(\Delta d/\Delta t)_l/(\Delta d/\Delta t)_b$ given in tables 1 and 2, part 1, and recognizing that the etch pit areas remain constant, from

$$\frac{S_b}{S_l} = \frac{(\Delta d/\Delta t)_b}{(\Delta d/\Delta t)_l} \cdot \sum_i C_{ib} \Big/ \sum_i C_{il}\,. \tag{9}$$

The specific energy loss for 5.6 keV-Ar^+-ions within the uncoated subsurface layer developed at pH = 6.2 was calculated according to [56] as $(\mathrm{d}E/\mathrm{d}x)_l \approx 400$ eV/nm for a density of $\varrho = 1.8$ g cm^{-3}, see section 3.3., part 1, and a composition of $SiO_2 \cdot 0.25\,BaO \cdot 0.25\,B_2O_3 \cdot 0.27\,H_2O$.

The calculation of the specific energy loss within the subsurface layer of the coated specimen developed with pH = 6.2 was based on the analysis results for C_{ml} given in table 4, see also section 3.3., part 1, and was obtained as $(\mathrm{d}E/\mathrm{d}x)_l = 620$ eV/nm; the rather small H_2O concentration was neglected for this calculation. Considering the density of the glass with $\varrho = 3.64$ g cm^{-3}, the specific energy loss of the bulk glass was calculated as $(\mathrm{d}E/\mathrm{d}x)_b = 670$ eV/nm.

Using these $\mathrm{d}E/\mathrm{d}x$ values and the experimental ratios of sputter rates and the respective concentrations of the glass and the leached subsurface layers (see section 3. and table 1, part 1, and table 4), the mean bond energy of the atoms within the leached layers was determined from equation (8) as 0.94 U_{Bl} for the uncoated and as 1.28 U_{Bl} for the coated SiO_2-rich subsurface layers developed at pH = 6.2. The results indicate that the material of the leached layer of the coated sample has a distinctly greater bond energy than that layer which was left uncoated during storage. It must be kept in mind, however, that these results may reflect the increase of the bond energy within the coated subsurface layer only

qualitatively because the different masses of the components within the glass were not taken into calculation, see [54 and 55]. Thus, it must be left open how far the value of the bond energy of fused silica, its density and specific energy loss was approached within the subsurface layer below the coating. It can be suggested that it was not yet reached because it was found, that the subsurface layers under investigation showed a further shrinkage when a higher temperature was applied, see section 4.4.2. A more precise investigation to draw conclusions on the absolute respective bond energies will require a further development of the theory and additional experiments as well.

The dE/dx values used above were calculated using an expression for the reduced stopping power given in [56] (see also [57] and the references given there) which is supposed to result in a better approximation for the keV energy range of the projectile ions than when Thomas-Fermi potentials were applied without corrections as in earlier calculations by which greater reduced stopping power values were obtained [39, 40 and 58]. It should be mentioned that a somewhat greater specific energy loss of $dE/dx \approx 700$ eV/nm for thin SiO_2 dip coatings was derived from the experiments in previous investigations [59] (for further discussions see [39 and 40]). The use of somewhat smaller stopping powers according to [32] would change the ratio of the specific energy losses used here by a few per cent at best, therefore, these differences are not of importance here.

From the analysis in section 3.3., part 1, and these considerations it is obvious that there are differences between the two subsurface layers with regard to compositions, the mean specific energy losses, therefore, and the mean bond energies. This means that the energy transfer mechanisms, both by elastic and inelastic collisions, will be different between the two subsurface layers and between these layers and the bulk glass. The differences in the mechanisms unavoidably contribute to the differences in the ionization coefficients for the bulk and for the two subsurface layers.

The matrix effect for IBSCA was smaller than for SIMS, see section 4.1. It obviously differs from that of SIMS according to tables 4 and 5. This difference lets suggest that the energy transfer mechanism in the collision cascades generated near the surface which causes the excitation of the emitted radiation is different from that for the ionization. This suggestion is supported by other results, see e. g. [50, 51, 60 and 61]. According to Kelly [51 and 61] this can be understood by a statistical model which involves that the neutral atoms which are ejected during sputtering in an excited state are formed in a single collision from the outermost layer of atoms only whereas the ionized sputtered atoms can be formed in quite different ways. The ejected ions, therefore, may reflect the bond breaking but in a different way than the excited neutral atoms [47 and 48]. Thus, the Si II intensity and the Si II in-depth profiles would reflect the change in the bonds much more than the Si I intensity given in figure 2b, part 1. It should be mentioned here that the radiation emitted by ionized Ba^+ atoms, e. g. the Ba II emission line at $\lambda = 413.07$ nm, showed for the subsurface layer developed with pH = 8.5 the very same in-depth dependence as the $^{138}Ba^+$ secondary ion current (the Si II and Ba II profiles are not shown here). The increase of the ionization within the subsurface layers can be understood qualitatively by a loosening of Si−O or Si−O−H bonds [47].

Also the Ba−O and the B−O bonds seem to be affected because the barium and boron ionization coefficients were increased by the introduction of hydrogen as can be concluded from the experimental results.

According to the considerations given in this section a difference between the matrix effects for SIMS and IBSCA can be assumed to exist generally for silica glasses of various compositions. The hydrated subsurface layers in particular will also have a distinct difference in composition and specific loss compared to the bulk.

Therefore, the different sputter rates observed may be taken to indicate hydrated subsurface layers. Especially the in-depth profiling with SIMS and IBSCA is unavoidably connected with these sputter quantities. The difference in the matrix effects, therefore, can also be generally used to detect changes of material properties. Such differences may be due to changes of the composition, the density of the material and of the bond energies connected with them. These changes can be correlated with measurements of other material properties too, as will be discussed in the sections 4.4.1. and 4.4.2.

4.3. Enhancement of the ionization coefficients used for qualitative analysis

As discussed in section 4.1. an enhancement of the Si^+ secondary ion yield was observed which was connected with the hydration of a subsurface layer of the SK 16 glass.

It can be derived from tables 1 and 2, see part 1, that for barium and boron the ratios Q_m^+ are always smaller than the ratios Q_m^I. This is due to the smaller matrix effect of IBSCA compared to that of SIMS. Therefore, the results given in section 3.1., part 1, also contain the information that within the hydrated subsurface material SIMS shows for the main glass components silicon, barium and boron a higher sensitivity than IBSCA and the difference of the in-depth profiles obtained with these two methods can be used to indicate hydration (also oxidation and

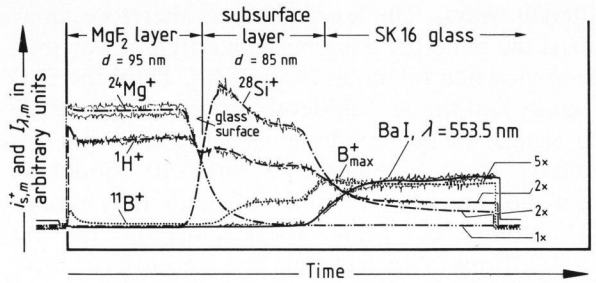

Figure 8. In-depth profiles of the $^{1}H^{+}$, $^{11}B^{+}$, $^{28}Si^{+}$ and $^{138}Ba^{+}$ currents and the intensity of the excited Ba I emission line at $\lambda = 553.55$ nm recorded after another thermal treatment at 340 °C for 12 h of the coated specimen, treated with a slurry of pH = 8.5 (see figure 2d in part 1 for comparison).

other composition changes could be studied by such a comparison, see section 4.2.).

An example for the application of the differences in the matrix effects between SIMS and IBSCA for a qualitative analysis is illustrated by figure 8. The in-depth profiles of this figure were recorded for the very same specimens as those given in figure 2d, part 1, but after an additional thermal treatment at 340 °C for 12 h. The $^{11}B^{+}$ secondary ion current in figure 8 shows a small relative maximum close to the interface of the subsurface layer and the bulk which was not observed in figure 2d, part 1. From the knowledge about the increase of the ionization coefficients p^{+} by hydration as discussed in section 4.1. it must be concluded that this maximum for boron indicates that during the second thermal treatment the hydrogen concentration near the interface was increased. The $^{11}B^{+}$ maximum appeared in spite of the decrease of the boron concentration within the interfacial layer by an interdiffusion of B^{+} ions with H_3O^{+} ions, because of the much greater p^{+} value caused by the introduction of H_3O^{+} ions. Furthermore, the shoulder of the B^{+} secondary ion current coincided with a decrease of both the $^{1}H^{+}$ and $^{28}Si^{+}$ secondary ion currents, see figure 8. This indicates that the exchange of hydrogen against boron from the bulk caused a decrease of the degree of hydration and of the ionization coefficients of silicon. Therefore, it can be concluded that the highest degree of hydration was reached within the subsurface layer in-between the MgF_2 layer and the $^{11}B^{+}$ shoulder. It is worth mentioning that the intensity of the Ba I line in figure 8 did not show a shoulder, different from what was recorded for the Ba^{+} secondary ion current prior to the second thermal treatment (figure 2d, part 1). This again illustrates the greater sensitivity of SIMS compared to IBSCA and can be understood by the peculiarities of the excitation, see section 4.2. It can also be derived that the ionization coefficients p_m^{+} seem to be very sensitive to hydrogen, regardless to whether hydrogen was introduced during the attack of an aqueous solution by interdiffusion or by other mechanisms. This can be derived from the in-depth profiles given in figure 2b, part 1. The penetration of hydrogen into the bulk, which was indicated in figure 2b by the $^{1}H^{+}$ signal, can be assumed to be due to a drift of hydrogen generated by a surface potential [24]. Most probably the discharging by low-energy electrons did not compensate this surface potential during the in-depth analysis of the profiles given in figure 2b, part 1; the other profiles did not show this effect. And different from figure 2a, part 1, the $^{11}B^{+}$ and $^{138}Ba^{+}$ secondary ion currents show a flat maximum beyond the interface during the ablation of the bulk. This maximum can be related qualitatively with the potential-induced drift of hydrogen to greater depths. Also it is most interesting to note that the abscissa of the small step of the silicon concentration indicated by the Si I emission line in figure 2b, part 1 (denoted by the arrow no. 1) does not coincide with the steepest slope of the $^{11}B^{+}$ or $^{138}Ba^{+}$ secondary ion current which occured at the interface with the bulk (denoted by the arrow no. 2). From the difference of the Si I intensity at these two positions it can be derived that the degree of hydration was distinctly smaller close to the bulk glass than in other parts of the leached layer. From this small step of the in-depth distributions it can be derived that a somewhat greater refractive index existed within that part of the layer positioned close to the bulk which was about 22 nm thick as can be calculated from figure 2b, part 1. Within the subsurface layers developed with pH = 8.5 such distinct steps of the Si I profiles were not observed, see figure 2d in part 1, indicating that there was a different in-depth decrease of hydration within the subsurface layer. Different from what was found for the specimen treated with a slurry of pH = 6.2, the SIMS profiles showed "shoulders" for Ba^{+} and B^{+} secondary ions.

4.4. Production parameters and properties of the subsurface layers

It was left open hitherto whether the formation of the different optical thicknesses and the respective different in-depth profiles can be correlated with production parameters. In particular, see table 4, the refractive index of the uncoated subsurface layer developed at pH = 6.2 was distinctly greater than that of the coated one. This was rather surprising because all the specimens were immersed together into the slurry at the same time and the duration of the surface attack was the same before some of them were coated. Furthermore, there was no "shoulder" observed for the $^{138}Ba^{+}$ and $^{11}B^{+}$ secondary ion currents during the SIMS in-depth analysis of the coated layer at pH = 6.2. This was different from what was found within the coated layer developed with pH = 8.5, see figure 2d in part 1.

Recognizing what was known already about the formation of subsurface layers during corrosion on

the surface of barium-containing and other glasses (see e. g. [1, 2, 5 to 10, 31, 42 and 62 to 64]) it was assumed that these unexplained changes occured during cleaning and the subsequent treatment. In particular it was expected that there was an influence of the duration of storage after cleaning.

In order to see whether there was an influence of the cleaning procedure, two uncoated specimens were prepared again which underwent the very same polishing process and were subsequently leached in a slurry with pH = 8.6 for 21 h at $\vartheta = 23\,°C$. The subsequent cleaning procedure was different, however. One sample was rubbed with deionized water only, whereas the other sample was cleaned by an ultrasonic-assisted procedure with an aqueous solution of pH = 8 at 57 °C which contained cleaning agents and during a second step trichlorethylene. Immediately after leaching and cleaning their surfaces showed the same spectral reflectance $R(\lambda)$ within the limits of error. According to the $R(\lambda)$ curves, the thickness of the layer on both the samples was the same and was calculated as 232 nm; their refractive index was also the same with $n = 1.445$. This low refractive index indicated that almost no barium was left within these subsurface layers. This observation was in agreement with the SIMS results and proved to be most important as will be discussed below.

Subsequently these differently cleaned specimens were stored in an exsiccator at room temperature ($\vartheta \leq 30\,°C$) for three months. After this storage the results of the SIMS and IBSCA measurements together with measurements of the spectral reflectance allowed further conclusions on the influence of the production parameters, also for the samples described already in the sections 3.1. to 3.3. in part 1 and 4.1. to 4.3. This will be discussed in the following sections 4.4.1. and 4.4.2.

4.4.1. Uncoated subsurface layers

According to the results of SIMS and IBSCA in-depth profiling, an interdiffusion between glass components of the bulk and the hydronium ions within the hydrated subsurface layer occured during the storage of the two uncoated samples treated at pH = 8.6 and cleaned as described in section 2.2., part 1. The Ba^+ and B^+ secondary ion currents recorded for these samples were comparable to those recorded in figures 2c and e, see part 1. An increase of the refractive indices of the two uncoated subsurface layers developed with pH = 8.6 from $n = 1.445$ to $n = 1.52$ and 1.515, respectively, was found to occur during storage. The thicknesses of the leached layers on these two samples were only slightly different after the storage, 268 and 254 nm. These small differences in the thicknesses and the refractive indices allow to conclude that the influence of the different cleaning procedures on the interdiffusion during storage was about the same.

After storage the refractive indices of the samples treated at pH = 8.6 were almost equal to the refractive indices of $n = 1.52$ and $n = 1.53$, respectively, which were found for the other uncoated subsurface layers developed with pH = 6.2 and pH = 8.5, respectively, as described in section 3., see table 3 in part 1. Therefore, it can be concluded that the uncoated samples analyzed as described in section 3., part 1, were also almost completely leached immediately after the interaction with the slurry and the cleaning and that an interdiffusion process during storage before the analysis had generated the observed in-depth profiles.

Another most important information on the ratios of the concentrations of barium and boron can be based on the knowledge of this interdiffusion process which attacks the bulk glass during storage. As can be seen from figures 2c and e in part 1, the change of the barium and boron concentrations occured at about the same depths at the interfaces between the bulk and the subsurface layers of both uncoated specimens. This indicates that there were no preferential reactions of one of these two components with the hydronium ions during storage. Therefore, the ratio for the concentrations of barium and boron within the subsurface layer after storage must be the same as within the bulk glass, with the concentration of boron about twice that of barium. The concentration of barium was analyzed with RBS, see section 3.3., part 1, as $C_{Ba} = 0.23 \cdot 10^{22}\,cm^{-3}$, therefore $C_B = 0.46 \cdot 10^{22}\,cm^{-3}$, see table 4.

The in-depth analyses and the refractive indices of the uncoated subsurface layers show that the activities of barium and boron approached almost equal values after a prolonged storage for the two samples considered here and for the samples described in the preceeding sections 3.1. to 4.3. However, it can be derived from the measurements that at least the thicknesses of the uncoated layers were distinctly different immediately after leaching when the leaching took place in different slurries, see sections 2.2., 3.2. and table 3, part 1. These differences in the thicknesses let conclude that the interaction of the glass surface with the different slurries resulted in different ratios of the total dissolution rates of the glass and the partial dissolution rates of the leaching process which develops the subsurface layer [63]. These different ratios in turn imply that a difference between the activities of the components of the slurry and those within the subsurface layer exists.

For the subsurface layers considered in the present investigations it can be assumed that a steady state was reached after an interaction with the slurries of 6 h, respectively 23 h. This steady state is characterized by a constant dissolution rate and a linear increase of the dissoluted glass volume, because the

activities of the attacking solution were kept constant (the dissolution rates often will show a parabolic time dependence for shorter interaction times, see e. g. [5, 9 and 65] and the discussion given in [31]).

From the considerations given in this section above and in section 3., part 1, it can be derived that the properties of the optical surfaces for the glass considered here may depend sensitively on variations in the chemical composition of adjacent phases and the activities of their components. It seems necessary to refer also to results reported by other authors for an understanding of the great variety of properties which can be found especially prior to coating. Some of the phenomena considered in the following were observed on the surfaces of other glasses and illustrate at the same time their importance for the optical fabrication in general. The conclusions drawn in this section on the consequences of the different activities and different ratios for the total and partial dissolution rates are of importance generally. This is because it is well-known from the glass electrodes that different phase-boundary potentials [66] and different interfacial potentials between the leached layer and the bulk glass exist for different activities of attacking solutions which are due to a different interdiffusion reaction through hydrated subsurface layers [67]. According to previous results [68 and 69], the degree of condensation of hydrated silica within the subsurface layer may depend also on the time of interaction during a subsequent "ageing" by immersion of the specimen into another aqueous solution with other activities of the components. During ageing the degree of condensation may be changed again and, therefore, the ratios of the dissolution rates may change, too. Accordingly the change of the optical thickness of the subsurface layer and the ratio of the dissolution rates were found to be linked together, see [63]. In particular when the sample is stored within a gaseous atmosphere the time-dependent changes of the properties of the subsurface layer will depend on the partial pressure of the water vapour and other gaseous components. The formation of non-volatile reaction products which were deposited on the surface was found to occur also during storage in gaseous atmospheres [3, 4, 9 and 14]. The degree of condensation close to the surface can be different from the deeper parts of the leached layers because a composition gradient can be induced by the adjacent phases. A different composition and homogeneous condensation in the layer close to the surface, therefore, can be connected with a change of the refractive index at the surface [6, 7, 9 and 70]. However, a partial ageing can be started also in small areas on the surface by fingerprints or droplets and can cause spots [3, 4 and 9]. The condensation of the hydrated silica in turn can influence the chemical resistivity against corrosion and it appears that the superposition of different reactions can occur. These phenomena in turn affect the mathematical treatment of the interdiffusion processes, see the discussions in [31 and 71]. Also other results obtained for thin silica-rich leached subsurface layers give support that a low-temperature condensation can take place [72 and 73], similarly to what would be expected for hydrous silica from [68 and 69]. For further considerations see also [74].

With respect to a lack of reproducibility in optical fabrication, it has to be emphasized here, that the dissolution rates can be changed drastically even by traces of impurities [75]. In any case, it may be important to know the activities of all of the components present in the slurry for a greater range of concentrations and how to select and to control them [63, 70 and 76].

Regardless of the way on which hydrogen was introduced into the hydrated subsurface layers considered here, it can be assumed that Si–O–H groups exist within these layers and that molecular water can be formed and can emanate during their condensation [10, 30, 71 and 77 to 82]. Experiments show that the concentration ratio of molecular water to Si–O–H groups is a function of the glass composition and water concentration in the base glass [80]. It has to be mentioned here that for other barium-containing glasses similar and most drastic changes of the material forming the hydrated subsurface layers were observed and a collapse of the leached network occured when the specimen was exposed to the air [7 and 42]. It was also found that pores can exist within the subsurface layers [42 and 83] which contain considerable amounts of molecular water; see also [29]. The desorption of this water was observed during drying, heating and during storage [42 and 83] within the vacuum prior to analysis [84].

It can be assumed that depending on the preconditioning a variety of different condensation equilibria can be possible for the atoms within subsurface layers considered here. This latter assumption can be given support by the findings described in [10] for other glasses which showed that the variety of bonds can be characterized by different activation energies, and also by the finding that the mean bond energies vary as discussed already in section 4.2. (the lowering of the bond energies is also reflected by a change of the hardness and the ablation rate during polishing [85]). Recognizing the different properties of the leached hydrated subsurface layers mentioned in section 3.3., part 1, and this section above, it is not astonishing, therefore, that the ratios of the concentration of the hydrogen atoms introduced into the network of the subsurface layers and that of the alkali atoms replaced by them were different for different glasses and the experimental parameters as temperature, pH value, partial pressure of gases, times of interaction and the activities of components present in the attacking solutions, see e. g. [26, 27 and 79 to 83] and the discussion given in [62, 71 and 85].

It can be derived that the size and the charge of the species during the transport through the subsurface layer for an interdiffusion reaction can vary, too. A continuous transport of mobile cations to the surface takes place through the subsurface layer when the steady state of glass dissolution is reached. This transport requires interdiffusing H_3O^+ ions for charge compensation. Otherwise a space charge would block the transport in a network of fixed anionic groups. Also molecular water can be introduced together with the H_3O^+ ions [26, 29, 30, 83 and 86]. The resulting interdiffusion coefficients, however, seem to be not influenced by the molecular water, and they depend on the mobility of the H_3O^+ ion and the interdiffusing ions only for some glasses, see e. g. [87]. The diffusion constants in general depend on the different mobilities of the ionic species involved in the interdiffusion, see e. g. [88 and 89] and the references given there. It is clear from the examples for variations of the atomic structure and the condensation discussed in section 4.4.2. and in this section above that the interdiffusion constants also must show a great variability.

On the other hand, the subsurface layer material can be porous and cracks can be formed also so that the transport of reactants between an aqueous solution and the bulk surface will occur with preference through these open paths [7, 10, 73 and 83]. An influence of the surface energies can result in a quite different structure of the porous layers inside or outside the attacking liquid [7], see also [11 and 12]. Moreover, the surface free enthalpies can depend on the temperature and can induce differences in the subsequent condensation reactions [83]. Phase separation also can occur and can change the interdiffusion mechanism and other properties of the leached layers [90 and 91]. The properties of the subsurface layers of another hydrated glass could be explained by a structure which consists of residual glass islands amongst a water-rich gel phase [92]. It will be difficult, however, to distinguish between the transport mechanisms through a network of fixed anionic groups and the transport through pores if there is a continuous transition between these transport mechanisms for the same glass depending on the thermal treatment, e. g. [73]. Similarly also the subsurface layers on the glass investigated in the present work can act as diffusion barriers, e. g. after the condensation at higher temperatures, $\vartheta = 240\,°C$ (see sections 4.2. and 4.4.2.). And from this finding it can be concluded that the mean diameter of the pores was reduced drastically by this treatment; cracks have not been observed. The mechanisms of dissolution of the glass and the resulting structure of the glass network can differ very much for the different optical glasses and the paths for the reacting species could also vary strongly. And furthermore it has to be recognized that often the final steady state of leaching and dissolution will not be reached with the parameters applied in fabrication.

From the in-depth analysis and the results of other work discussed so far, it can be summarized that the properties and their changes of the subsurface layers considered here will be determined by the following: The pH value and the activities of the components dissolved in the slurry, including impurities, determine the thickness and composition of the silica-rich subsurface layers after the steady state of leaching is reached (which implies constant dissolution rates). These activities of the components contained in the slurry and other agents adjacent to the glass surface also determine the degree of condensation of the subsurface layers which is characteristic for the glass and the processing conditions. The degree of condensation determines the concentration of Si–O–H groups, the water content and the physical properties such as the atomic densities, the refractive index, and the mean bond energies of the network atoms. The change of the activities by the interdiffusion reaction during storage can result in a time-dependent and an in-depth-dependent change of the degree of condensation and, therefore, a change of the refractive index. Especially the time dependence of the changes induced during storage also must be considered for the interpretation of the surface analysis results and for a selection and a control of the processing parameters in optical fabrication.

The formation of subsurface layers by leaching can cause measurable tensile stresses, even cracking of the glass surface can occur. The leaching consists of a superposition of a variety of interactions when pores and cracks exist and when inhomogeneous or phase-separated subsurface layers were developed. Such phenomena can be disclosed often only by surface analysis methods. The analysis will be often unavoidable since there exist almost no data on the interdiffusion processes and the free enthalpies of reaction for the processing parameters applied in optical fabrication.

It can be derived from a comparison of the present results with other results published recently [3 and 4] that also for much thinner subsurface layers on SK 16 glass the same mechanisms of interaction with adjacent phases apply.

Depending on the attacking phases and the glass composition, a variety of phenomena can influence, therefore, the properties of the subsurface layers and in particular the properties of the optical surfaces prior to coating. The most important phenomenon for optical fabrications appears to be the formation of hydrated silica-containing subsurface layers. Finally it should be mentioned that it cannot be excluded that the composition and the structure of the subsurface layers can be influenced also by reactions with crystals of the polishing grains [93 and 94]. However,

reactions occuring during polishing were not in the scope of the present investigations.

4.4.2. Coated subsurface layers

The knowledge of the phenomena which determine the properties of the uncoated optical surfaces can be used also to understand the hitherto unexplained origin of differences within the optical properties of the coated subsurface layers. As was described in section 4.4.1., it could not be explained why there were differences within the optical properties of the subsurface layers of the coated and the uncoated samples though both underwent the very same pretreatment. The knowledge about the influence of the duration of storage and the thermal treatment allows to conclude on the origin of these differences as follows: Both the uncoated samples developed with pH = 6.2 and 8.5 were stored for a few weeks prior to analysis. This storage was long enough that barium and boron could be introduced in considerable quantities by interdiffusion with the hydrogen contained within the leached layer.

The samples which underwent a pretreatment with a slurry of pH = 6.2 were coated within a few hours after the cleaning. During the coating process and the subsequent thermal treatment the hydrated subsurface layers condensed to a silica-rich layer. Such layers can act as diffusion barriers, see e.g. [14]. Accordingly it can be concluded that the samples treated at pH = 6.2 were quickly condensed to such a state during coating and the subsequent thermal treatment so that they represented a diffusion barrier for barium and boron. Due to the condensation of this subsurface layer during coating a shrinkage to $d = 130$ nm occured, see table 4. The comparison of the concentrations of hydrogen before and after shrinkage (see table 4) shows that almost all the hydrogen, presumably condensed to water, was lost. The in-depth profiles showed that there was no silicon from the bulk glass introduced into the subsurface layer by diffusion during the condensation. Therefore, the increase of the silicon concentration within this subsurface layer during condensation to $2.2 \cdot 10^{22}$ cm^{-3}, see section 3.3., part 1, and table 4, must be ascribed to a decrease of the mean distance of the silicon atoms within the subsurface layer after condensation. For further results on swelling and shrinkage of hydrated subsurface layers, see [6, 7 and 79].

The "shoulders" for the in-depth profiles of the Ba^+ and B^+ secondary ion currents within the leached layers of the coated samples treated at pH = 8.5, see figures 2d, part 1, and 8, also can be explained by an accelerated condensation during the coating procedure: It can be assumed that barium and boron were extracted completely from the subsurface layer immediately after the leaching with pH = 8.5 because this was the case with pH = 8.6 too, see section 4.4.1. Therefore, the "shoulders" of barium and boron represent the frontiers of the interdiffusion in that state in which the thermal treatment stopped the interdiffusion reaction by a quick condensation. Different from the uncoated specimen – treated at pH = 8.5 – the equilibrium for the interdiffusion reaction was not yet reached in this state. The outer part of the layer formed a silica-rich diffusion barrier. This can be concluded from the in-depth profiles given in figure 8 which show that the outer part of the layer of the sample leached at pH = 8.5 remained boron-free during another thermal treatment with 340 °C for 12 h. Before this second thermal treatment a relatively great water content was observed, see table 5, and in agreement with what was discussed in section 4.4.1. a shrinkage from 150 to 88 nm was observed after the treatment during coating, see table 5. After the second thermal treatment at $\vartheta = 340$ °C the sputter rate was reduced again and $(\Delta d/\Delta t)_b/(\Delta d/\Delta t)_l = 1.05$ resulted instead of 0.93 before. This indicates another increase of the mean bond energies due to condensation of the leached material.

There are numerous publications on the corrosion of glasses and on the formation of subsurface layers during the interaction with aqueous solutions and on the changes of properties induced by subsequent processing. It is impossible to refer here on even the most important of these papers and, therefore, the effects and the special properties of subsurfac layers discussed here do not represent a complete overview. On the other hand, it cannot be expected that such an overview would contain the special answers required to solve a problem in fabrication of optical surfaces. This is because of the many parameters and the variations which could induce measurable changes of the properties of the optical surfaces after polishing and cleaning and after coating. Furthermore, it has to be noted, that glasses do not form ideal solutions [95]. The free enthalpies of reaction mostly cannot be calculated exactly because there is a lack of data for the partial free enthalpies of formation, and the mobilities of the glass constituents are not known under fabrication conditions. Thus, it is mostly not possible to calculate the yields of the interdiffusion and dissolution reactions and the partial and total dissolution rates quantitatively [4]. Therefore, it will be often unavoidable to investigate how individual glasses react with the aqueous solutions and adjacent phases during processing, similarly to what has been presented in the present paper: The results of analyses which disclose the influence of the change of production parameters on the chemical and other processes and the optical properties must be compared with each other. From this comparison and the basic results of the interaction of glass surfaces with the adjacent phases it can be concluded on the dissolution rates quantitatively [4] and adequate measures can be taken in the fabrication to improve

the quality and the reproducibility of the properties of the optical surfaces.

From the results given in section 4.4.1. and from those of other authors it can be concluded that the formation of hydrated subsurface layers should be avoided completely for any of the optical glasses. This conclusion must be drawn because of the numerous parameters which eventually influence the properties of the hydrated subsurface layers during processing and in particular after polishing and before coating. However, the formation of the subsurface layers might be unavoidable if special fabrication processes must be applied. In this case the activities of the components present in the slurry during polishing must be kept constant and the duration of the interaction of the optical surface with the slurry or with a humid atmosphere must be kept short after polishing. Also the duration of storage before coating must be kept as short as possible for glasses developing subsurface layers with properties as described in section 4.4.1. Moreover, it seems promising to condense these hydrated subsurface layers to such a degree by heating after cleaning that they block interdiffusion reactions and reactions with the atmosphere as it could be done with the subsurface layers on SK 16 glass studied here.

For a selection of the production parameters it has to be taken into account also, that the surface energy and the composition of the subsurface layer can influence the properties of the coatings too; for a review of these problems see e.g. [96].

5. Summary and conclusions

It was shown by analysis with SIMS, IBSCA and RBS that during the prolonged interaction of the $SiO_2-BaO-B_2O_3$ glass surfaces with slurries of pH values in the range $6 < pH < 9$ for a few hours and after cleaning a decrease of the silicon concentration and an almost complete exsolution (leaching) of barium and boron occur within subsurface layers which were 80 to 190 nm thick.

The in-depth analysis of hydrogen in these layers with NRA showed that barium and boron were partly replaced by hydrogen during an interdiffusion reaction with the slurry. The comparison of the NRA, RBS, SIMS and IBSCA results with each other showed an increase of the ionization coefficients p^+ for positively charged secondary ions and a decrease of the excitation coefficients $\alpha_{\lambda,m}$ of sputtered neutral atoms in the hydrated material relative to the bulk glass. These special matrix effects of SIMS and IBSCA which are different from those of the bulk material can be used to detect and to characterize hydrated subsurface layers. It could be concluded that the activities of the components within the subsurface layers change when the activities of the components in the slurry were changed.

Presumably a part of the hydrogen was introduced as H_3O^+ ions, another part as molecular water. However, it could not be excluded that molecular water was formed by condensation of Si–O–H groups which were generated during the interaction with the slurry before storage. An interdiffusion reaction between this water available within the subsurface layers and the components of the bulk glass was observed to occur after cleaning during storage of the optical surfaces in gaseous environments. It took a few weeks to attain the final yield which indicates that the interdiffusion constant was rather small. Therefore, a variety of in-depth distributions were found in various samples depending on the duration of the intervals between the different treatments and on the duration of storage before analysis. It must be recognized, however, that the condensation process can be superimposed at the same time on the interdiffusion, inducing changes of the interdiffusion process again. Furthermore, it must be taken into account that a part of the molecular water could evaporate during storage in the air and prior to analysis when vacuum was applied.

The hydrated subsurface layers of the glass considered in the present work consisted essentially of a network in which the concentration of silicon atoms of the bulk glass was reduced during leaching. This decrease of the silicon concentration can be described as a "swelling" which was due to an increase of the mean distances between the silicon atoms. This swelling was linked with the formation of Si–O–H groups, the introduction of water and the existence of molecular water cannot be excluded. Relative changes of the mean bond energies of the atoms within the hydrated subsurface layers (obtained by variations in the processing) could be derived from the differences in the sputter rates and the calculated specific energy losses for the various subsurface layers.

A prolonged thermal treatment at elevated temperatures ϑ with $230\,°C \leq \vartheta \leq 340\,°C$ resulted in an increase of the mean bond energies of the atoms within these subsurface layers which was connected with an emanation of water and an increase of the atomic density of Si. Thus silica-rich subsurface layers were formed by condensation with about the same silicon concentration as fused silica. They contained almost no hydrogen or other components when this thermal treatment took place immediately after leaching. These subsurface layers acted as diffusion barriers for barium and boron.

The mean bond energies derived from the sputter experiments showed a distinct increase with decreasing hydrogen concentration. It is proposed, therefore, to characterize the equilibrium of hydration and condensation by the mean bond energies derived from sputter experiments.

From the comparison with other work on hydrated subsurface layers it can be concluded that the

properties of the leached subsurface layers can vary strongly for different glass compositions and fabrication parameters. Mostly no diffusion constants of the elements and free enthalpies of reactions are available for the processes under fabrication conditions. Therefore, it is not possible generally to predict the existence and the properties of subsurface layers for any other fabrication processes and other glasses, and the application of surface analysis methods in the fabrication is unavoidable for studying the influence of the various fabrication processes.

The present results illustrate that generally various analysis methods and measurements of the optical and other properties must be applied to complement each other for the quantitative analysis of the in-depth changes of the chemical composition, of the structure and of the physical properties of the hydrated subsurface layers. Only the combined application of the various methods allows to understand and to control the influence of the fabrication parameters. For the investigations of the chemical and physical processes it can be useful or even unavoidable to intentionally produce much thicker subsurface layers than commonly produced by the fabrication processes. This is because for thicker layers the various influences can be distinguished more easily by the analysis methods because of their limited in-depth resolution. Additional experiments in which the fabrication parameters are changed intentionally can be unavoidable to separate the superimposed influences of different interaction mechanisms from each other.

The subsurface layers contribute to the change of the optical properties by coating and to other properties of the uncoated or coated optical surfaces. The properties of the subsurface layers can be very sensitive against the activities of the components within adjacent phases. Their formation, therefore, should be avoided completely. If this will be not feasible, the activities of the components of the slurry and other adjacent phases applied in processing before coating must be kept constant at least. Also the duration of interaction with the adjacent phases must be always the same and must be kept as short as possible. Whether these conditions will be sufficient to reproduce the properties of the subsurface layers depends on the glass composition and other details of the processing, too. This must be carefully investigated if a high degree of reproducibility of the optical properties is required.

*

This work has been supported by the Bundesministerium für Forschung und Technologie, Bonn (FRG) (Förderungskennzeichen 13 N 5226). Nevertheless the authors are responsible for the contents. They are grateful to Mrs. U. Erb, Mrs. B. Sommer, Mrs. M. Neumann, Schott Glaswerke, Mainz, and Dipl.-Phys. M. Braun, Dr. H. Dobler, Carl Zeiss, Oberkochen, and Mr. Hermann Bach, Armsheim, for much practical assistance and experimental contributions and calculations.

6. References

[1] Schröder, H.: Über Einflüsse der Politur auf die Oberflächenkorrosion von Glas. Glastech. Ber. **22** (1948/49) no. 18, p. 424–425.

[2] Günther, K. H.: Colour variations of AR coatings caused by a leached layer on the substrate. Appl. Opt. **20** (1981) no. 1, p. 48–53.

[3] Bach, H.: Analysis of surface layers. In: Walter, H. (ed.): DGaO/SPIE symposium on optical surface technology, Garmisch-Partenkirchen (FRG) 1983. Conf. proc. p. 113–128.

[4] Bach, H.: Analysen an Oberflächenschichten und Belägen für die Fertigung optischer Flächen. T. 1/2. Vak.-Tech. **33** (1984) no. 3, p. 67–77; no. 4, p. 99–108. [Rev. Glastech. Ber. **58** (1985) no. 6, 85R0795.]

[5] Hench, L. L.; Clark, D. E.: Physical chemistry of glass surfaces. J. Non-Cryst. Solids **28** (1978) no. 1, p. 83–105. [Rev. Glastech. Ber. **52** (1979) no. 11, 79R2395.]

[6] Schröder, H.: Die Eigenschaften von optischen Gläsern mit chemisch veränderter Oberfläche. T. 1/2. Z. tech. Phys. **22** (1941) no. 2, p. 38–43; [Rev. Glastech. Ber. **19** (1941) no. 9, p. 304.] **23** (1942) no. 8, p. 196–208. [Rev. Glastech. Ber. **21** (1943) no. 9, p. 208.]

[7] Schröder, H.: Reflexverminderung und Konstitution des Glases. Glastech. Ber. **20** (1942) no. 6, p. 161–166.

[8] Schröder, H.: Physikalisch-chemische Eigenschaften von Glasoberflächen. Glas-Email-Keramo-Tech. **14** (1963) no. 5, p. 161–168.

[9] Kinosita, K.: Surface deterioration of optical glasses. In: Wolf, E. (ed.): Progress in optics. Vol. IV. Amsterdam: North-Holland Publ. Co. 1965. p. 87–143.

[10] Dunken, H. H.: Reaktivität and optische Eigenschaften von Glasoberflächen. Wiss. Z. Friedrich-Schiller-Univ. Jena, Math.-Naturwiss. R. **32** (1983) no. 2/3, p. 263–283. (2. Int. Otto-Schott-Kolloquium.)

[11] Weyl, W. A.: Structure of subsurface layers and their role in glass technology. J. Non-Cryst. Solids **19** (1975) no. 1, p. 1–25.

[12] Kreidl, N. J.: Glass surfaces then and now. J. Non-Cryst. Solids **49** (1982) p. 331–338. [Rev. Glastech. Ber. **57** (1984) no. 4, 84R0694.]

[13] Baucke, F. G. K.: Equilibria of functional groups of glass surfaces with cations in contacting solutions. In: The glassy state, Proc. 7th All-Union Conference, Leningrad 1981.

[14] Bach, H.: Oberflächen- und Dünnschichtanalysen an Glasoberflächen und Oberflächenbelägen. T. 1//Oberflächen- und Tiefenprofilanalysenverfahren. T. 2//Bewertung der Oberflächen- und Tiefenprofilanalysenverfahren und die gleichzeitige Anwendung mehrerer Verfahren. T. 3//Anwendung der Analysenverfahren in Entwicklung und Produktion. Glastech. Ber. **56** (1983) no. 1, p. 1–18; no. 2, p. 29–46; no. 3, p. 55–62.

[15] Bach, H.: Preparation and analysis of bulk specimens and thin film using the universal ion beam etching device IEU 100 from BALZERS. In: Pfefferkorn, G. (ed.): 12. Kolloquium des Arbeitskreises für elektronenmikroskopische Direktabbildung und Analyse von Oberflächen, Tübingen 1979. Vol. 12/1. p. 277–306.

[16] Günther, K. H.; Hauser, E.; Hobi, G. et al.: A novel etching unit applicable for depth profiling with SIMS and IIR. In: Benninghoven, A.; Giber, J.; Laszlo, L. et al. (eds.): Secondary ion mass spectrometry – SIMS III. Berlin, Heidelberg, New York: Springer 1982. p. 97–101.

[17] Oechsner, H. (ed.): Thin film and depth profile analysis. Berlin, Heidelberg, New York: Springer 1984.

[18] Coburn, J. W.: The influence of ion sputtering on the elemental analysis of solid surfaces. Thin Solid Films **64** (1979) p. 371–382.

[19] Bach, H.; Baucke, F. G. K.: Investigation of glasses using surface profiling by spectrochemical analysis of sputter-induced radiation. Pt. 1//Surface profiling technique with high

in-depth resolution. Pt. 2//Baucke, F. G. K.; Bach, H.: Field-driven formation and electrochemical properties of protonated glasses containing various proton concentrations. J. Am. Ceram. Soc. **65** (1982) no. 11, p. 527–533, 534–539. [Rev. Glastech. Ber. **57** (1984) no. 10, 84R1486, 84R1487.]

[20] Werner, H. W.: Theoretical and experimental aspects of secondary ion mass spectrometry. Vacuum **24** (1975) p. 493–504.

[21] Tolk, N. H.; Tsong, I. S. T.; White, C. W.: In situ spectrochemical analysis of solid surface by ion beam sputtering. Anal. Chem. **49** (1977) no. 1, p. 16A–18A, 22A, 24A–26A, 28A, 30A.

[22] Oechsner, H.; Rühe, W.; Stumpe, E.: Comparative SNMS and SIMS studies of oxidized Ge and Gd. Surface Sci. **85** (1979) p. 289–301.

[23] Slodzian, G.: Dependence of ionization yields upon elemental composition, isotopic variations. In: Benninghoven, A.; Giber, J.; Laszlo, J. et al. (eds.): Secondary ion mass spectrometry – SIMS III. Berlin, Heidelberg, New York: Springer 1982. p. 115–123.

[24] Bach, H.; Hallwig, D.: Analysis of sodium on glass surfaces disturbed by ion-beam induced absorption currents. Radiat. Eff. **81** (1984) p. 129–153. [Rev. Glastech. Ber. **58** (1985) no. 11, 85R1434.]

[25] Werner, H. W.; Morgan, A. E.: Charging of insulators by ion bombardment and its minimization for secondary ion mass spectrometry (SIMS) measurements. J. Appl. Phys. **47** (1976) no. 4, p. 1232–1242.

[26] Lanford, W. A.; Davis, K.; Lamarche, P. et al.: Hydration of soda-lime glass. J. Non-Cryst. Solids **33** (1979) no. 2, p. 249–266. [Rev. Glastech. Ber. **53** (1980) no. 7, 80R1285.]

[27] March, P.; Rauch, F.: Soda-lime glasses studied by ion-induced nuclear reactions. Nucl. Instrum. Methods **B 15** (1986) p. 516–519.

[28] Tsong, I. S. T.; Houser, C. A.; Tong, S. S. T.: Depth profiles of interdiffusing species in hydrated glasses. Phys. Chem. Glasses **21** (1980) no. 5, p. 197–198.

[29] Smets, B. M. J.; Lommen, T. P. A.: SIMS and XPS investigation of the leaching of glasses. Verres Réfract. **35** (1981) no. 1, p. 84–90. [Rev. Glastech. Ber. **54** (1981) no. 11, 81R1551.]

[30] Ernsberger, F. M.: Electrical transport of protons in solids. Glastech. Ber. **56K** (1983) Vol. 2, p. 963–968.

[31] Scholze, H.: Chemical durability of glasses. J. Non-Cryst. Solids **52** (1982) p. 91–103.

[32] Ziegler, J. F.: The stopping and ranges of ions in matter. Vol. 5. Oxford: Pergamon Press 1977.

[33] Chu, W.-K.; Mayer, J. W.; Nicolet, M.-A.: Backscattering spectrometry. New York: Acad. Press 1978.

[34] Bach, H.: Das Ionenstrahlätzen – Anwendungsmöglichkeiten bei elektronenmikroskopischen Untersuchungen und der Analyse von Festkörperoberflächen. Beitr. elektronenmikrosk. Direktabb. Oberflächen **5** (1972) p. 479–553.

[35] Hofmann, S.; Sanz, J. M.: Depth resolution and quantitative evaluation of AES sputtering profiles. In: Oechsner, H. (ed.): Thin film and depth profile analysis. Berlin, Heidelberg, New York: Springer 1984. p. 141–158.

[36] Pulker, H. K.; Jung, E.: Correlation between film structure and sorption behaviour of vapor deposited ZnS, cryolite and MgF_2 films. Thin Solid Films **9** (1971) p. 57–66.

[37] Simonov, B. M.; Pelipas, V. P.; Balagurov, A. Y. et al.: Determination of moisture contents of thin films of MgF_2, ZnS, and Na_3AlF_6 by means of infrared spectroscopy. Inorg. Mater. **16** (1980) no. 3, p. 293–295.

[38] Bach, H., Mainz: Unpubl. results.

[39] Bach, H.: Determination of bond energy of silica glass by means of ion sputtering investigations. Nucl. Instrum. Methods **84** (1970) p. 4–12. [Rev. Glastech. Ber. **45** (1972) no. 8, R72–1137.]

[40] Bach, H.; Kitzmann, I.; Schröder, H.: Sputtering yields and specific energy losses of Ar ions with energies from 5 to 30 keV at SiO_2. Rad. Eff. **21** (1974) p. 31–36. [Rev. Glastech. Ber. **49** (1976) no. 10, 76R1365.]

[41] Kempf, J. E.; Wagner, H. H.: In-situ laser measurements of sputter rates during SIMS/AES in-depth profiling. In: Oechsner, H. (ed.): Thin film and depth profile analysis. Berlin, Heidelberg, New York: Springer 1984. p. 87–102.

[42] Günther, K. H.; Hauser, E.; Kramer, R.: Diffusion study of thin film formation by leaching optical glasses in an acidic solution. Thin Solid Films **89** (1982) p. 277–283.

[43] Müller, K. H.; Oechsner, H.: Quantitative secondary neutral mass spectrometry analysis of alloys and oxide-metal-interfaces. Mikrochim. Acta (1983) Suppl. 10, p. 51–60.

[44] Ahn, J.; Perleberg, C. R.; Wilcox, D. L. et al.: Electron beam effects in depth profiling measurements with Auger electron spectroscopy. J. Appl. Phys. **46** (1975) p. 4581–4583.

[45] Barcz, A.; Domanski, M.; Wojtowicz-Natanson, B.: Current density effects on secondary ion emission from multicomponent targets. In: Benninghoven, A.; Giber, J.; Laszlo, J. et al. (eds.): Secondary ion mass spectrometry – SIMS III. Berlin, Heidelberg, New York: Springer 1982. p. 134–139.

[46] Garret, R. F.; MacDonald, R. J.; O'Connor, D. J.: The energy dependence of the ionisation coefficient in SIMS. In: Benninghoven, A.; Okano, J.; Shimizu, R. et al. (eds.): Secondary ion mass spectrometry – SIMS IV. Berlin, Heidelberg, New York: Springer 1984. p. 66–69.

[47] Williams, P.: On mechanisms of sputtered ion emission. Appl. Surf. Sci. **13** (1982) p. 241–259.

[48] Gerhard, W.; Plog, C.: Secondary ion emission by nonadiabatic dissociation of nascent ion molecules with energies depending on solid composition. Z. Phys. B – Condens. Matter **54** (1983) p. 59–70, 71–86.

[49] Ohwaki, T.; Taga, Y.; Satta, K.: Secondary ion emission from Si subjected to oxygen ion bombardment. In: Benninghoven, A.; Okano, J.; Shimizu, R. et al. (eds.): Secondary ion mass spectrometry – SIMS IV. Berlin, Heidelberg, New York: Springer 1984. p. 35–37.

[50] Thomas, G. E.: Bombardment induced light emission. Surf. Sci. **90** (1979) p. 381–416.

[51] Kelly, R.: Statistical model for the formation of excited atoms in the sputtering process. Phys. Rev. **B 25** (1982) no. 2, p. 700–712.

[52] Yu, L. M.; Reuter, W.: Matrix effect in SIMS analysis using an O_2^+ primary beam. J. Vac. Sci. Technol. **17** (1980) no. 1, p. 36–39.

[53] Anderson, H. H.; Bay, H. L.: Sputtering yield measurements. In: Behrisch, R. (ed.): Sputtering by particle bombardment I. Berlin, Heidelberg, New York: Springer 1981. p. 145–218.

[54] Sigmund, P.: Sputtering by ion bombardment//Theoretical concepts. In: Behrisch, R. (ed.): Sputtering by particle bombardment I. Berlin, Heidelberg, New York: Springer 1981. p. 9–71.

[55] Sigmund, P.; Oliva, A.; Falcone, G.: Sputtering of multicomponent materials//Elements of a theory. Nucl. Instrum. Methods **194** (1982) p. 541–548.

[56] Steinbrüchel, C.: A simple formula for low-energy sputtering yields. Appl. Phys. **A 36** (1985) p. 37–42.

[57] Wilson, W. D.; Haggmark, L. G.; Biersack, J. P.: Calculations of nuclear stopping, ranges, and straggling in the low-energy region. Phys. Rev. **B 15** (1977) p. 2458–2468.

[58] Bach, H.: Abtragraten und spezifische Energieverluste von 5,6 keV-Edelgasionen an Kieselglas. Z. Naturforsch. **27a** (1972) no. 2, p. 333–338.

[59] Bach, H.: Zur Bestimmung der Reichweiten von beschleunigten Ionen in dünnen Oxidschichten. Z. Angew. Phys. **28** (1970) no. 4, p. 239–244.

[60] White, C. W.; Simms, D. L.; Tolk, N. H. et al.: Effects of nonradiative de-excitation of excited sputtered atoms near silicon and silicon dioxide surfaces. Surface Sci. **49** (1975) p. 657–663.

[61] Kelly, R.: Mechanism of emission of SiI, SiII and SiIII from Si

which is ion bombarded in the presence of oxygen. Nucl. Instrum. Methods **209/210** (1983) p. 509–512.

[62] Belyustin, A. A.: Concentration distribution of ions in the surface layers of alkali silicate glasses treated with aqueous solutions. Sov. J. Glass Phys. Chem. **7** (1981) no. 3, p. 169–188. [Rev. Glastech. Ber. **56** (1983) no. 1, 83R0066.]

[63] Schröder, H.: Über die Angreifbarkeit des Glases durch Lösungen mit pH-Werten nahe 7. Glastech. Ber. **26** (1953) no. 4, p. 91–97.

[64] Schröder, H.: Verfahren zur Durchlässigkeitserhöhung und Reflexverminderung von Glas od. dgl. Stoffen. DBP 821 828. Kl. 32 b; Gr. 6/50. Pat. ab 2. 10. 1948, ausgeg. 18. 9. 1952.

[65] Richter, T.; Frischat, G. H.; Borchardt, G. et al.: Short time leaching of a soda-lime glass in H_2O and D_2O. Phys. Chem. Glasses **26** (1985) no. 6, p. 208–212.

[66] Boksay, Z.; Bouquet, G.: The pH dependence and an electrochemical interpretation of the dissolution rate of a silicate glass network. Phys. Chem. Glasses **21** (1980) no. 3, p. 110–113. [Rev. Glastech. Ber. **54** (1981) no. 4, 81R0618.]

[67] Baucke, F. G. K.: The origin of the glass electrode response. In: Wright, A. F.; Dupuy, J. (eds.): Proc. NATO Advanced Study Institute on Glass, curr. issues. Dordrecht, Boston, Lancaster: Nijhoff 1985. p. 481–505.

[68] Willstätter, R.; Kraut, H.; Lobinger, K.: Zur Kenntnis der Monokieselsäure und Dikieselsäure. XII. Mitt. über Hydrate und Hydrogele. Ber. Dtsch. Chem. Ges. **62** (1929) p. 2027–2034.

[69] Schwarz, R.: Das Siliciumdioxyd und seine Hydrate. Z. Elektrochem. **34** (1926) no. 9, p. 415–419.

[70] Hähnert, M. (In the original paper the name is erroneously written as "Henert"); Rauschenbach, B.: Surface layers of silicate glasses. Sov. J. Glass Phys. Chem. **9** (1983) no. 6, p. 487–493.

[71] Scholze, H.: Bedeutung der ausgelaugten Schicht für die chemische Beständigkeit: Untersuchungen an einem Kalk-Natronsilicatglas. Glastech. Ber. **58** (1985) no. 5, p. 116–124.

[72] Ivanovskaya, I. S.; Belyustin, A. A.; Shul'ts, M. M. et al.: Distribution of sodium in the surface layers of sodium silicate glasses after interaction with aqueous solutions. Sov. J. Glass Phys. Chem. **1** (1975) no. 2, p. 139–143. [Rev. Glastech. Ber. **49** (1976) no. 11, 76R1500.]

[73] Rudakova, S. E.; Krasov, V. A.; Agafonova, O. V.: Structure and composition of the surface layer formed on aluminosilicate E-type glass after acid treatment. Sov. J. Glass Phys. Chem. **8** (1982) no. 3, p. 237–241. [Rev. Glastech. Ber. **57** (1984) no. 10, 84R1488.]

[74] Hench, L. L.: Glass surfaces 1982. J. Phys. **43** (1982) suppl: Colloque C 9, p. C 9-625–C 9-636.

[75] Geffcken, W.; Berger, E.: Grundsätzliches über die chemische Angreifbarkeit von Gläsern. II. Glastech. Ber. **16** (1938) no. 9, p. 296–304.

[76] Elmer, T. H.: Role of acid concentration in leaching of cordierite and alkali borosilicate glass. J. Am. Ceram. Soc. **68** (1985) no. 10, p. C-273–C-274.

[77] Moriya, Y.; Nogami, M.: Hydration of silicate glass in steam atmosphere. J. Non-Cryst. Solids **38 & 39** (1980) p. 667–672.

[78] Ernsberger, F. M.: The nonconformist ion. J. Am. Ceram. Soc. **66** (1983) no. 11, p. 747–750.

[79] Scholze, H.; Helmreich, D.; Bakardjiev, I.: Untersuchungen über das Verhalten von Kalk-Natrongläsern in verdünnten Säuren. Glastech. Ber. **48** (1975) no. 12, p. 237–247.

[80] Wu, C.-K.: Nature of incorporated water in hydrated silicate glasses. J. Am. Ceram. Soc. **63** (1980) no. 7/8, p. 453–457. [Rev. Glastech. Ber. **55** (1982) no. 4, 82R0752.]

[81] Olbert, B. H.; Doremus, R. H.: Infrared study of soda-lime glass during hydration and dehydration. J. Am. Ceram. Soc. **66** (1983) no. 3, p. 163–166. [Rev. Glastech. Ber. **58** (1985) no. 1, 85R0004.]

[82] Scholze, H.; Bakardjiev, I.: Entalkalisierung von Glasoberflächen durch saure Wasserbehandlung. Glastech. Ber. **50** (1977) no. 11, p. 281–285.

[83] Bunker, B. C.; Arnold, G. W.; Beauchamp, E. K. et al.: Mechanisms for alkali leaching in mixed-Na-K silicate glasses. J. Non-Cryst. Solids **58** (1983) no. 2/3, p. 295–322. [Rev. Glastech. Ber. **59** (1986) no. 2, 86R0152.]

[84] Pantano, C. G. jr.: Surface and in-depth analysis of glass and ceramics. Am. Ceram. Soc. Bull. **60** (1981) no. 11, p. 1154–1163, 1167. [Rev. Glastech. Ber. **55** (1982) no. 11, 82R2343.]

[85] Izumitani, T.: Polishing, lapping, and diamond grinding of optical glasses. In: Tomozawa, M.; Doremus, R. H. (eds.): Treatise on materials science and technology. Vol. 17: Glass II. New York: Acad. Press 1979. p. 115–172.

[86] Bartholomew, R. F.; Tick, P. A.; Stookey, S. D.: Water/glass reactions at elevated temperatures and pressures. J. Non-Cryst. Solids **38 & 39** (1980) p. 637–642.

[87] Doremus, R. H.; Babinec, A.; D'Angelo, K. et al.: Electrolysis of soda-lime silicate glass in water. J. Am. Ceram. Soc. **67** (1984) no. 7, p. 476–479.

[88] Frischat, G. H.: Ionic diffusion in oxide glasses. Bay Village, Aedermannsdorf: Trans Tech Publ. 1975. [Rev. Glastech. Ber. **49** (1976) no. 3, 76R0345.]

[89] Kaneco, T.: An ion exchange model of glass leaching. J. Mater. Sci. Lett. **4** (1985) p. 631–634.

[90] Tomozawa, M.; Capella, S.: Microstructure in hydrated silicate glasses. J. Am. Ceram. Soc. **66** (1983) no. 2, p. C-24–C-25.

[91] Doremus, R. H.; Mehrotra, Y.; Lanford, W. A. et al.: Reaction of water with glass//Influence of a transformed surface layer. J. Mater. Sci. **18** (1983) p. 612–622. [Rev. Glastech. Ber. **58** (1985) no. 1, 85R0064.]

[92] Schäfer, J.; Schaeffer, H. A.: Leaching of alkali silicate glasses – formation of hydrated layers, surface- and diffusion-controlled kinetics. Riv. Stn. Sper. Vetro **14** (1984) no. 5, p. 79–82. [Rev. Glastech. Ber. **59** (1986) no. 10, 86R0737.]

[93] Kaller, A.: Einfluß der chemischen, kristallographischen und physikalischen Eigenschaften der Poliermittel beim Polieren des Glases. Silikattechnik **34** (1983) no. 1, p. 15–17. [Rev. Glastech. Ber. **57** (1984) no. 3, 84R0505.]

[94] Optical Society of America: The science of polishing. Tech. dig. conf. on science of polishing, spring conference on applied optics, Monterey, CA (USA) 1984.

[95] Vogel, W.: Glaschemie. 2nd ed. Leipzig: VEB Deutscher Verlag für Grundstoffindustrie 1979. p. 103–136.

[96] Pulker, H. K.: Coatings on glass. Amsterdam: Elsevier 1984.

87R0072